Topoclimate buffers floristic diversity from macroclimate in temperate mountain forests.

Jeremy Borderieux[1], Emiel De Lombaerde[2], Karen De Pauw[2], Pieter Sanczuk[2], Pieter Vangansbeke[2], Thomas Vanneste[2], Pieter De Frenne[2], Jean-Claude Gégout[1], Josep M. Serra-Diaz [1,3].

1. Université de Lorraine, AgroParisTech, INRAE, UMR Silva, 54000 Nancy, France
2. Forest & Nature Lab, Department of Environment, Ghent University, Geraardsbergsesteenweg 267, 9090 Gontrode, Belgium
3. Eversource Energy Center and Department of Ecology and Evolutionary Biology, University of Connecticut, Storrs, CT, United States of America

Orcid ID:

Jeremy Borderieux : 0000-0003-3993-1067

Emiel De Lombaerde : 0000-0002-0050-2735

Karen De Pauw : 0000-0001-8369-2679

Pieter Sanczuk : 0000-0003-1107-4905

Pieter Vangansbeke : 0000-0002-6356-2858

Thomas Vanneste : 0000-0001-5296-917X

Pieter De Frenne : 0000-0002-8613-0943

Jean-Claude Gégout : 0000-0002-5760-9920

Josep M. Serra-Diaz: 0000-0003-1988-1154

Corresponding author: Jeremy Borderieux: jeremy.borderieux@agroparistech.fr

Abstract

Microclimates strongly influence the composition and diversity of forest plant communities. Recent studies have highlighted the role of tree canopies in shaping understory thermal conditions at small spatial scales, especially in lowland forests. In mountain forests, however, the influence of topography in environmental conditions (e.g. topoclimate) is ought to also influence plants' perceived temperature. Understanding how topography and canopies interactively affect understory temperature is key to identifying stable refugia that could shelter cold-adapted forest specialist species under climate change.

Here we report on growing season understory temperatures using 48 loggers in contrasting topographic features of a mid-range mountain valley spanning from 475 m.a.s.l. to 1203 m.a.s.l. in the Vosges Mountains (NE France). We disentangle the relative importance and the effects of topography vs. canopies in determining local temperatures. We then evaluate how topography and canopy-induced variation in temperature drive plant community composition and richness in 306 floristic surveys distributed across the studied mountain valley.

Our results show that topography outweighed canopy cover in explaining growing season understory temperatures. Regardless of canopy, the daily mean temperature of the growing season in south-facing ridges was 1.5 °C (CI: ± 0.88 °C) warmer than shaded valley bottoms, while dense canopies cooled temperatures by 0.5 °C (CI: ± 0.48 °C) compared to open canopies. Topoclimate explained community composition as much as elevation and was the only significant predictor of species richness. Cold topoclimates harbored 30% more species than the average species richness across our plots. This increase in species richness was explained by an increase of cold-adapted species, both forest specialist and generalist species.

Our findings highlight a stronger role of topography compared to canopy cover on community composition in mountain forests via topoclimatic cooling of north-facing slopes and valley bottoms. The importance of topographic features to explain temperature cooling and diversity underpins their role as present and future microrefugia.

Keywords

Community ecology, forest, topoclimate, microclimate, topography, temperature, climatic refugia, diversity, understory vegetation.

1. Introduction

The study of topography influences on vegetation has fascinated ecologists for more than 150 years (Johnston et al., 1848), and has further gained relevance in the context of the 21st century climate warming (Ashcroft, 2010; Dobrowski, 2011; IPCC, 2021; Lenoir *et al.*, 2017). Species distribution and climatic conditions are often modeled at a coarse resolution (typically 1 km or coarser), and thereby fail to capture local variation of climate at fine grains (Franklin *et al.*, 2013) : for instance, the topoclimate shaped by topography and the microclimate shaped by forest canopy (Bramer *et al.*, 2018; De Frenne *et al.*, 2021; Kemppinen *et al.*, 2023). Given that these factors can attenuate warm macroclimate temperatures, the study of the effects and interactions between topography and forest canopy are key to identify areas of climate stability in a warmer future (Ashcroft, 2010; De Frenne *et al.*, 2021; Haesen *et al.*, 2023; Hannah *et al.*, 2014).

Variations in aspect can create contrasting topoclimates as slopes oriented to the equator receive more solar radiation. As a result, southwest-facing slopes in northern hemisphere mountains display warmer mean temperatures, longer growing seasons and shorter snow cover durations (Ashcroft *et al.*, 2008; Davis *et al.*, 2019; Rita *et al.*, 2021). The physical properties of air also interact with topographic features such as hydrological basins (McLaughlin *et al.*, 2017), valley bottoms and sinks, and create local areas of cold and dense air pooling that decouple local conditions from the regional climate (Gudiksen *et al.*, 1992; Pastore *et al.*, 2022). , thus creating topographic refugia (Dobrowski, 2011). The topoclimate created by these terrain features interacts with the microclimate induced by forest canopies and jointly determines the understory temperature experienced by forest organisms. Canopy shading and evapotranspiration lead to an overall decrease of temperature throughout the year, compounded by a buffering of high summer temperatures compared to open-air, and an increase in winter temperatures due to insulation, (De Frenne *et al.*, 2021; Zellweger, Coomes, *et al.*, 2019). These buffering effects are apparent and well documented in temperate lowland forests, but their relative importance in contrast to elevation and topography is less known, and current evidence has not reached consensus (Macek *et al.*, 2019; Vandewiele *et al.*, 2023).

Canopy cover cooling of understory temperature has strong effects on forest communities. This is evidenced by the increases in the average thermal optimum of the species present (a proxy of species' affinity to climate) in forests where tree canopy was removed (De Frenne *et al.*, 2013; Dietz *et al.*, 2020; Richard *et al.*, 2021) and where warmer understory temperatures are predicted (Zellweger *et al.*, 2020). This sheltering of cold-adapted species by a dense canopy needs to be compared with the sheltering provided by topography in mountain forests, as topographical refugia are likely to offer longer-term buffering of temperature. Topographic refugia also harbor cold-adapted flora and host populations of species outside their expected climatic range (Ellis & Eaton, 2021; Finocchiaro *et al.*, 2023; Macek *et al.*, 2019). In addition, understanding the characteristics of the

sheltered species can also bring new insights, an increase of forest generalists for example demonstrates that topoclimate can mimic understory conditions of dense forests.

Here we assessed the effects and relative importance of elevation, topography and canopy cover on *in situ* measured understory temperatures and plant community composition and richness. After accounting for the elevation gradient, we specifically asked: (1) Does topography (aspect and topographic position) outweigh canopy in explaining understory temperature, (2) does topography and canopy-induced variation in microclimate determine community richness and mean species thermal optimum? (3) Are plant habitat preference and climatic affinity related to specific temperatures?

2. Materials and Methods

2.1. Study Area

Our study region (221 km^2) is delineated by the basin of the Thur River, located in one of the southmost valleys of the Vosges Mountain range in France (Figure 1). The Vosges are characterized by a continental climate with harsh winters and short and stormy summers. Its mean annual temperature ranges from 6 °C to 10°C and precipitation ranges from 800 to 2,000 mm $year^{-1}$(period 1970-2000, Météo France weather stations IGN, 2013). The Thur River basin is on the warm and dry end gradient of the Vosges Mountains (IGN, 2013). Forests cover 76% of the Vosges, which transitions from mixed oak stands and monospecific *Picea abies* stands to mixtures of *Picea abies*, *Abies alba* and *Fagus sylvatica* as elevation increases IGN, 2013). The soil of our study region is mostly shallow loam and sand with coarse elements. The most acidic soils are found at higher altitudes because of the dominance of needles in the humus and the lower temperature at mountaintops (IGN, 2013; Piqué *et al.*, 1994; Thomas *et al.*, 1999). The topography is highly variable, with an elevation ranging from 400 to 1424 m.a.s.l (but forest occurrence stops past 1250 m.a.s.l) with high topographic heterogeneity (Figure 1).

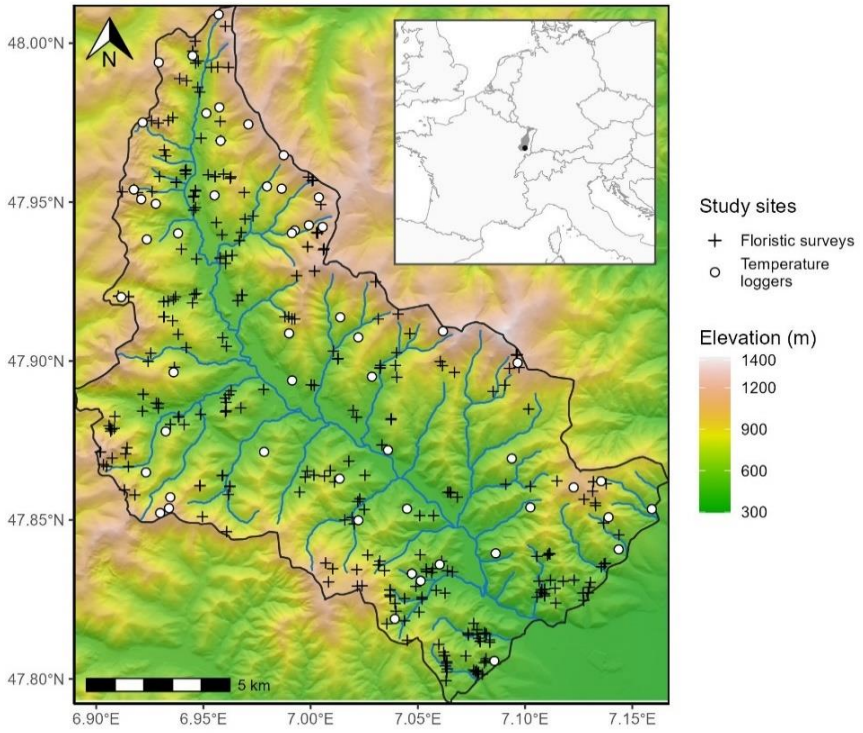

Figure 1: Map of the study area (black outline) with the location of the temperature loggers (white circles) and the floristic surveys (black crosses). The colored scale represents elevation above sea level, in meters, obtained from a 25-m spatial resolution digital elevation model. Hillshade effects have been added to visualize the terrain. The inset shows the Vosges Mountain range (grey) and the location of the studied valley (black point) in western Europe.

2.2. Temperature Predictors

We used 25-meter resolution digital elevation models to extract elevation (m.a.s.l.), slope and aspect and to calculate topographical indices, heat load and topographic position (IGN, 2017). We handled spatial data with the '*raster*' and '*sf*' packages (Hijmans, 2020; Pebesma, 2018), and all the later analyses were carried on with R.4.2.2 (R Core Team, 2019). We used '*ggplot2*' and '*ggspatial*' packages for data visualization (Dunnington & Thorne, 2020; Wickham, 2011). We computed the heat load index (McCune & Keon, 2002) using the 'spatialEco' R package (Evans & Murphy, 2021). The heat load index ranges from 0 to 1 (least to most incoming solar radiation) contingent on the slope orientation and shading from nearby topographic features. The topographic position index is the relative position of the cell in the shortest trajectory between a ridge and a drainage basin end, ranging from 0 (valley bottom) to 1 (ridge, Piedallu *et al.*, 2023).

We obtained the 'tree cover density' from the 2018 product of the Copernicus monitoring service as a proxy for local canopy closure (Copernicus, 2018; Sannier *et al.*, 2023). This product consists of a 10-meter resolution percentage of canopy presence within the pixel (ranging from 0 to 100%) and was successfully used before to model microclimate buffering by canopy (Haesen *et al.*, 2021). This product was correlated with our field measurements of canopy closure (see below, 2.3 Temperature sampling). We rescaled this

product to match the 25-m resolution of our other maps using bilinear interpolation (Hijmans, 2020). We rasterized (25-meter resolution) a 20-meter precision map of French forest to create a mask of the forested area of our study region, in order to limit our analysis and temperature projection to the forest of the region (IGN, 2019).

2.3. Temperature Sampling

We created a stratified sampling scheme to capture forest understory microclimate variability (Lembrechts *et al.*, 2021; Schweiger *et al.*, 2016). We created 8 elevation strata (spanning 20 m intervals) separated by 102 m ranging from [468 - 488] to [1184 - 1204] m a.s.l., aimed to control for the lapse rate (Lembrechts *et al.*, 2021), as it is the main driver of temperature in the study area. Inside each of these strata, we defined 8 types of plots: 4 plots of below and above the median canopy cover of our study area (90% canopy cover) with a south or a north-facing slope (defined as lower or higher than 0.75 heat load index). These 4 plots had moderate topographic position indices (between 0.2 and 0.8) and slope (10° < slope < 25°), to avoid confounding their effects with the canopy cover and heat load effects. Additionally, we defined 2 plots with contrasting topographic position indices (lower than 0.2 and higher than 0.8) under high canopy cover and moderate slope. Lastly, we defined 2 plots with contrasting slopes: one flat (slope < 10°) and one steep (slope > 25°) under high canopy cover and moderate topographic position.

Of the initial 64 theoretical plots spanning the 8 strata, only 59 of the defined situations occurred, mostly because we lacked low topographic position indices (valley bottom) in high elevation classes. We randomly selected one pixel for each plot and stratum located in public forests. We repeated this random drawing 10,000 times and kept the set of plots that maximized the mean minimum distance between plots to reduce spatial autocorrelation.

We established the 59 temperature loggers in May 2021 and recorded their location with a GNSS receiver (Trimble TDC600, accuracy= ± 2 m undercover). We placed every logger in public forests to avoid legal constraints (public forest makes up 80% of the forested area in our study region), with no constraints regarding accessibility. We measured canopy closure (0-100%) by visual observation in a 25-meter radius around the logger. We also estimated canopy cover (0-100%) with a planar picture of the canopy using a smartphone placed on top of the logger and the '*Glama'* application (Tichý, 2016). Plots tagged as low canopy cover were placed accordingly by selecting sites with less than 50% canopy closure as computed by '*Glama*'. The visual estimation of canopy closure (25-meter radius) was significantly correlated with the remote sensed tree density (R^2 of the linear relationship = 30.0%, Figure S1), but a weak and non-significant correlation was found with the picture analyzed by '*Glama*' (Figure S1).

We recorded air and soil temperatures with TMS-4 loggers (resolution= 0.0625 °C, accuracy= ±0.5 °C) protected with a radiation shield (Wild *et al.*, 2019). The loggers recorded temperature every 15 minutes until August 2022. We used air temperature 15 cm

above the soil surface because it is the most representative temperature experienced by understory plants. We cleaned the time series with the '*myClim*' R package (Man *et al.*, 2023). We calibrated the loggers beforehand for a range of -20 °C to +40 °C by placing them in a freezer and drying oven along with a T-type thermocouple (accuracy= ±0.2 °C). From the recorded period, we focused on the growing season, from 01/04/2023 to 15/08/2023, as it is the most critical period for plant growth. Out of the 59 loggers, 11 were either malfunctioning, stolen, destroyed by animals or displayed erroneous values and were discarded. We checked the capacity of our final sample to cover the variability of our study region following the PCA-based approach of Lembrechts *et al.*, (2021). Our final sampling was able to cover the variability of the valley, except for extreme values of low canopy cover and the unusual valley bottoms of high elevations. The loss of loggers was evenly distributed over plot types, except for the low canopy cover that suffered the most losses (Figure S2).

2.4. Floristic and Species Characteristic Dataset

We compiled floristic surveys performed (during the growing season) by students and professors covering soil and climatic transects of the region between 2009 and 2022 (average year= 2015.6). All plots were surveyed for all vascular plant species in the herb layer (smaller than 1 m) and their percentage ground cover was visually estimated. We had 306 floristics surveys in total across the study region. Floristic surveys were performed in 20 x 20 m squares (400 m^2) with the GPS position (recorded with built-in tablet GPS; accuracy= ± 10 m) as the center. We used this position to extract elevation, heat load index, topographic position index and canopy cover for every survey. We harmonized taxonomy to the TaxRef V13 standard (Gargominy, 2022). We focused on herbaceous species in the analysis to focus on community dynamics that may reflect shorter-term climate and are less influenced by management than trees or shrubs.

We used the thermal optimum species' value from ClimPlant V.1.2 (Vangansbeke *et al.*, 2021). These thermal optima are computed from the mean annual temperature within the range of species obtained from Europe-extent distribution atlases. Out of the 348 unique recorded species, 30 were assigned a thermal optimum value, covering 90.0% of the occurrences of the whole floristic dataset. We averaged the thermal optimum of every species (without weighting for abundance) of a given survey to obtain the Community Thermal Index (hereafter CTI), which quantifies the thermal preference of the whole community (Borderieux *et al.*, 2023; Vangansbeke *et al.*, 2021). We calculated species richness of a plot as the number of recorded species whether they had an associated thermal optimum in the database or not. By doing so, we wanted to include rare species that were not included in ClimPlant so that our specific richness is representative of the species pool of our study region. We also assigned a pH optimum value obtained from a bioindication database to each species (Gégout *et al.*, 2005), and averaged (not weighted by abundance) it to obtain a bioindicated pH per plot.

We used the EuForPlant regional list of forest plant species (Heinken *et al.*, 2022) to assess species habitat affinity. We assigned to each species one of the following affinities: (1.1) species of closed forest (1.2) species that occur in forest edges and openings (2.1) Species that primarily occur in forests but also found in cultural landscapes and forest remnants (2.2) species of open habitats that occur in forest exclusively through opening and early succession. We excluded species of open vegetation (classified "O") because of their low number of occurrences (42). In total, 274 species were assigned to an affinity class, covering 85.7% of the occurrences.

2.5. Understory Temperature Modeling

We aggregated the 15-minute frequency time series of the recorded temperature of the growing season 2022 to daily mean and maximum temperature. First, we removed values lower than the 5^{th} centile of the day and values higher than the 95^{th} centile to avoid biasing results due to logger malfunction or a brief burst of sunshine on a logger. We then averaged the mean or maximum daily temperature to obtain one unique value per logger, the mean daily and maximum daily temperature of the growing season.

We used a linear model to predict mean and maximum daily temperature of the growing season with elevation, heat load index, topographic position index and remote sensed canopy density as explanatory variables. We preferred remote-sensed canopy cover over the *in-situ* measurements which allowed us to map the temperature models over the entire study area, and thus infer the understory temperature of floristic surveys (mostly without canopy closure records). We additionally fitted two linear models with the field measured canopy closure (25 m radius observation and planar photography) instead of the remotely sensed measurement to test different methods of canopy closure estimations (Table S2, Table S3). The exceed in warming due to radiation can be amplified when canopy cannot intercept light, thus, we tested an interaction between heat load index and canopy closure and retained the interaction in the final model if found significant (Davis *et al.*, 2019).

The mean understory temperature model (R^2= 92.2%) allowed us to map the contribution of elevation (i.e., lapse rate), map the topoclimate (heat load index and topographic position) and the microclimate (canopy density) separately to the mean understory temperature (Figure 2). We mapped the lapse rate by using only the intercept and the elevation parameter. We mapped the contribution of topography cooling compared to the warmest situation (heat load index and topographic position index equal to 1) assuming a median canopy cover (90%) and using the two topographic indices. We mapped the contribution of canopy cover by multiplying its parameter by the tree density product, this projection is however extrapolated for the 20% of pixels with a canopy closure lower than 79%.

2.6. Floristic Composition Analyses

The soil of our study region can display very different nutrition status and acidity, which can impact both the richness and composition of a community (Degen et al., 2005; Koerner et al., 1997; Zellweger et al., 2015). In addition, soil pH is also negatively correlated with elevation. To account for soil acidity, we first fitted a linear model to predict species richness and CTI with bioindicated pH as the only predictor. These models had a significant R^2 of 32.6% and 21.5%, respectively. We then summed the mean species richness or CTI to the residual of the corresponding bioindicated pH model to obtain the corrected value. The corrected values allow comparison between communities with bioindicated pH considered equal.

We used a linear model to predict the corrected species richness and CTI with the contribution to mean understory temperature of elevation, topoclimate and microclimate as predictors (the unit of every predictor is thus °C). The parameters of these two models (species richness and CTI) are shown in Table 2. We discretized our results to better illustrate the control of the significant predictors of the model. We split the 306 surveys into three classes with an equal number of surveys, distributed in "cold", "intermediate" and "warm" classes. We tested the difference in species richness and CTI between these classes with Wilcoxon rank-sum tests (Rey & Neuhäuser, 2011).

We tested the assumption of normality and homoscedasticity of the residuals of the microclimatic model, the species richness and the CTI model following (Zuur & Ieno, 2016), and we tested the significant difference from 0 of the estimated parameters with a Wald test. We partitioned the variance of the predictors of all the models with the '*modEvA*' package (Barbosa *et al.*, 2013).

3. Results

3.1. Environmental determinant of the understory microclimate

The growing season (GS) temperature of 2022 was above average (mean GS temperature of the period 2005-2020=13.2°C, mean GS temperature=11.6 °C, Markestein weather station (1,184 m a.s.l), (Météo France, 2024)), as a result, the mean daily temperature of the understory (15 cm above the soil surface) was 14.6 °C and spanned between 11.9 °C to 17.5 °C for the higher (1203 m a.s.l) and lower (475 m a.s.l) elevation sensors, respectively. The mean daily maximum temperature of the GS was 19.3 °C and reached a maximum of 24.7 °C for the lowest elevation plots. Elevation was the primary driver of mean temperature variability, with a lapse rate estimated at -0.68 °C $100m^{-1}$ (Table 1). The heat load index– contingent on aspect and slope – was the second driver of mean temperature, which can vary up to 1°C between low and high radiation slopes (Table 1). Topographic position had a lesser effect on temperature: the mean temperature was 0.56° C lower in the bottom of a valley compared to ridges (Table 1). Lastly, canopy closure (remotely sensed) cooled understory temperatures. An increase of 20% of total canopy cover

298 resulted in a decrease of 0.57° C (Table 1). The lapse rate explained 87.4% of the variability
299 in mean temperature, the topographic factors (heat load and topographic position index)
300 3.95%, and canopy cover accounted for 0.82%. The R^2 of the linear model was 92.2%.

301 The same predictors except for topographic position were significant in the mean
302 daily maximum temperature model. The heat load index had a higher contribution (21.5%)
303 in the maximum temperature compared to the mean temperature model, daily maxima
304 varied for 3.3°C between low and high heat load indices (Table S1).

305 Canopy cover visually estimated in a 25-meter radius was not significant in predicting
306 mean temperature (Table S2). Immediate canopy cover (smartphone photography) above
307 the logger was significant in explaining mean temperature with an interaction with heat load
308 index, low immediate canopy cover in high radiation slopes displayed warmer mean
309 temperature (Table S3).

310 *Table 1: Estimated parameters, their standard error and p-values of the predictors included*
311 *in models of the daily mean growing season temperature. The range of the predictors in*
312 *the calibration dataset and their effect size on the temperature (range * estimate) are*
313 *displayed. The percentage of explained variation per type of predictor is included. P-values*
314 *were obtained with a Wald test on parameters. Heat load and topographic position have no*
315 *units, refer to the methods for their calculation.*

Predictor	Type of predictor	Estimate	Standard error	Range	Effect size (°C)	Explained variation (%)	P-value
Intercept (°C)		21,1	1,11				<10-4
Elevation (m a.s.l)	Elevation	-0.00684	0.000311	475 : 1203	-4.98	87.4	<10-4
Heat load index (n.u)	Topoclimate	1.53	0.333	0.335 : 0.951	0.945	3.95	<10-4
Topographic position (n.u)	Topoclimate	0.656	0.276	0.147 : 1	0.56	3.95	0.0220
Canopy closure (%)	Microclimate	-0.0272	0.0115	79.0: 100	-0.57	0.817	0.0229

316

317 The spatial variation of elevation, topography and canopy closure reveals complex
318 and fine-grained contributions to the forest understory climate (Fig. 2). We mapped the
319 individual contributions of elevation (Figure 2.a), topoclimate (heat load index and
320 topographic position summed; Figure 2.b) and canopy cover (i.e., microclimate; Figure 2.c)
321 in the study area. We represented topoclimate as a cooling effect compared to a baseline
322 location of a south-facing valley top (heat load index =1, topographic position=1) (Figure
323 2.b). The baseline for canopy cooling of temperature was 0% canopy closure (as pixels
324 displayed the whole 0-100% range), however, the range of microclimatic cooling from our
325 model is 79% to 100% (80% of the pixel, Figure 2.c). We observed strong effects on understory

temperatures caused by steep spatial differences in elevation, topography and fine-grained canopy cover (Figure 2.d). We used this map and model to predict the mean understory temperature and the contribution of the three components described above for further community composition analyses.

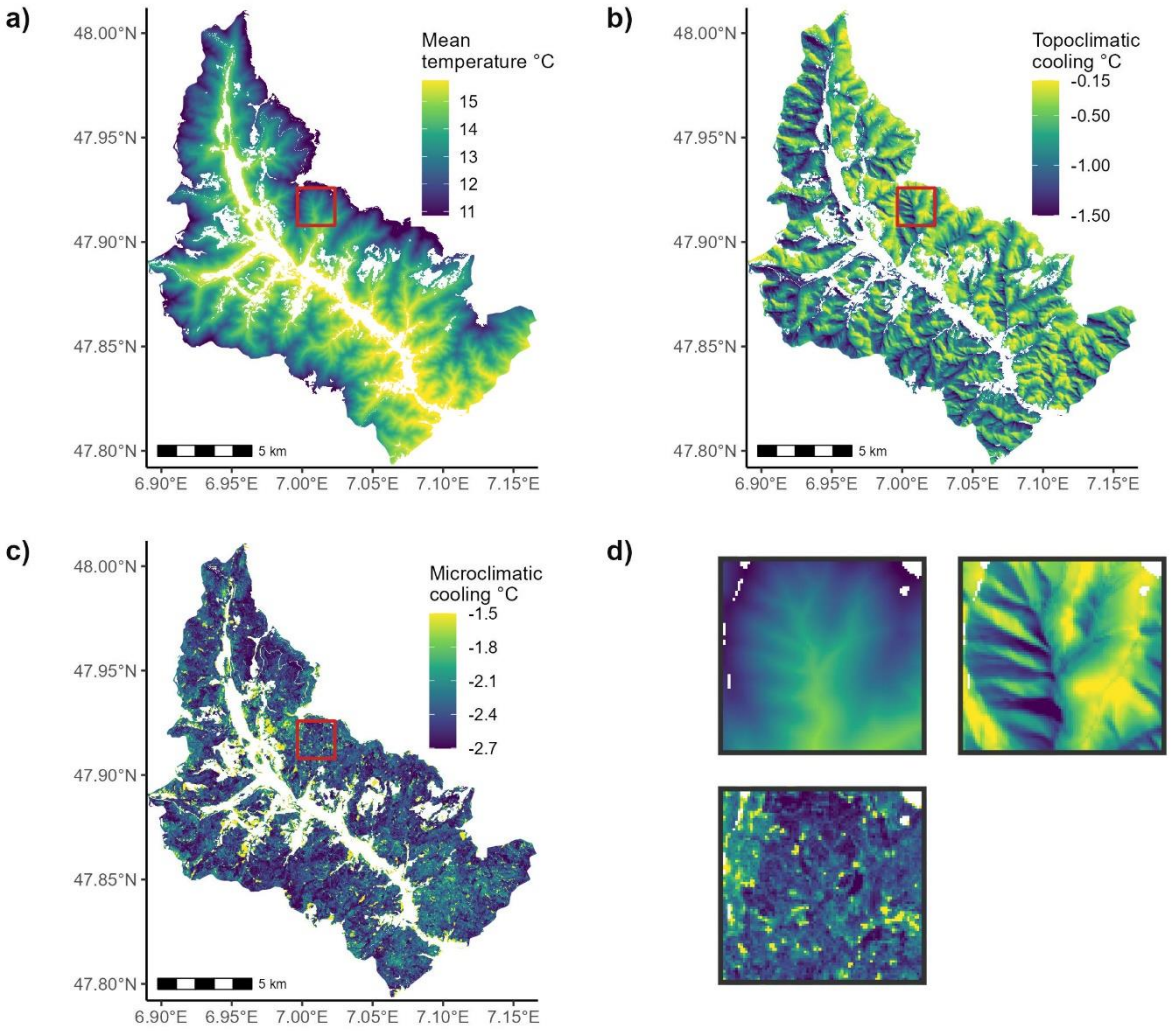

Figure 2: a) Elevation induced change in mean growing season understory temperature of the growing season (lapse of -0.68°C 100 m^{-1}), assuming a canopy closure of 90% and no effect from topography. b) mean understory temperature cooling induced by topography (heat load and topographic position, i.e. topography) assuming an average canopy cover (90%), compared to the warmest situation (south-facing ridges). c) mean understory temperature cooling induced by canopy closure (i.e. microclimate) assuming no effect from topography. We restrained the minimal cooling to -1.5°C, however some pixels displayed lower values up to 0°C due to low to no canopy closure. d) 2 km per 2 km zoomed inset of the red square of the other panels, their color gradient corresponds to the color scale presented in the other panels a-c, respectively. Blank pixels represent land covers other than forests or forests outside of the study region. Linear model R^2: 92.2%.

3.2. Microclimatic Determinants of the Floristic Composition

Floristic surveys harbored on average 19 herbaceous species (s.d. 10.7), and the mean community thermal index (CTI) was 7.8 (s.d. 0.55). pH was strongly correlated with CTI (R^2=28.3%) and species richness (R^2=32.6%). More acidic soils had less diverse and cold-adapted communities. We accounted for this relationship by extracting the residual of a linear model predicting CTI or species richness with pH as the sole predictor (see methods). After accounting for soil effects, elevation-induced change in temperature was the main predictor of CTI, but it did not significantly explain species richness (Table 2). The microclimate was not a significant predictor in any of the two models (Table 2). Topoclimate was the sole significant predictor of species richness, and it significantly explained CTI. The contribution of topoclimatic cooling to the explained variability of CTI (4.64%) was comparable to the explained variability by elevation (4.6%). We focused the subsequent community analysis around topoclimate cooling effects, as canopy cooling did not significantly explain the species richness nor CTI.

*Table 2: Estimated parameters, their standard error and p-values of the predictors of the specific richness and community thermal index (CTI) linear models. The range of the predictors and their effect size on the community predicted variable (range * estimate) are displayed. Both species richness and CTI have previously been corrected for their correlation with soil pH. The P-value is obtained by a Wald test on the parameter.*

Model	Predictor	Estimate	Standard error	Range	Effect size	P-value	Explained variation (%)	R^2 (%)
Species richness	Intercept (°C)	9.71	7.73			0.21		7.7
	Lapse rate (°C)	0.324	0.33	12.6: 18.5	1.91	0.324	0.93	
	Topography cooling (°C)	-6.91	1.54	-1.55 : -0.13	-9.78	<10-4	6.76	
	Canopy cooling (°C)	0.682	2.35	-2.72: -1.31	0.958	0.771	0.018	
Community thermal index (°C)	Intercept (°C)	6.83	0.407			<10-4		9.2
	Lapse rate (°C)	0.076	0.017	12.6 : 18.5	0.449	<10-4	4.6	
	Topography cooling (°C)	0.355	0.081	-1.55 : -0.13	0.503	<10-4	4.64	
	Canopy cooling (°C)	-0.00586	0.123	-2.72 : -1.31	-0.00822	0.962	0.0063	

We divided the 306 floristic surveys into cold, intermediate and warm topoclimatic classes each comprised of 102 surveys based on topography-induced cooling. The cold topoclimatic class displayed 23 species on average, while the two other classes displayed 18.5 species on average (Figure 3.a). This difference of approximately 5 species was

significantly different (Figure 3.a). The mean CTI of the cold topoclimatic class was 7.7 °C, which is significantly lower by 0.19°C than the CTI of the two other classes (Figure 3.b). No such differences were found when using microclimatic (canopy) cooling was used to create the classes (Figure S3). This discretization of the dataset displayed similar patterns as those observed in an alternative analysis using the continuous predictors of the linear model (Table 2, Figure S4).

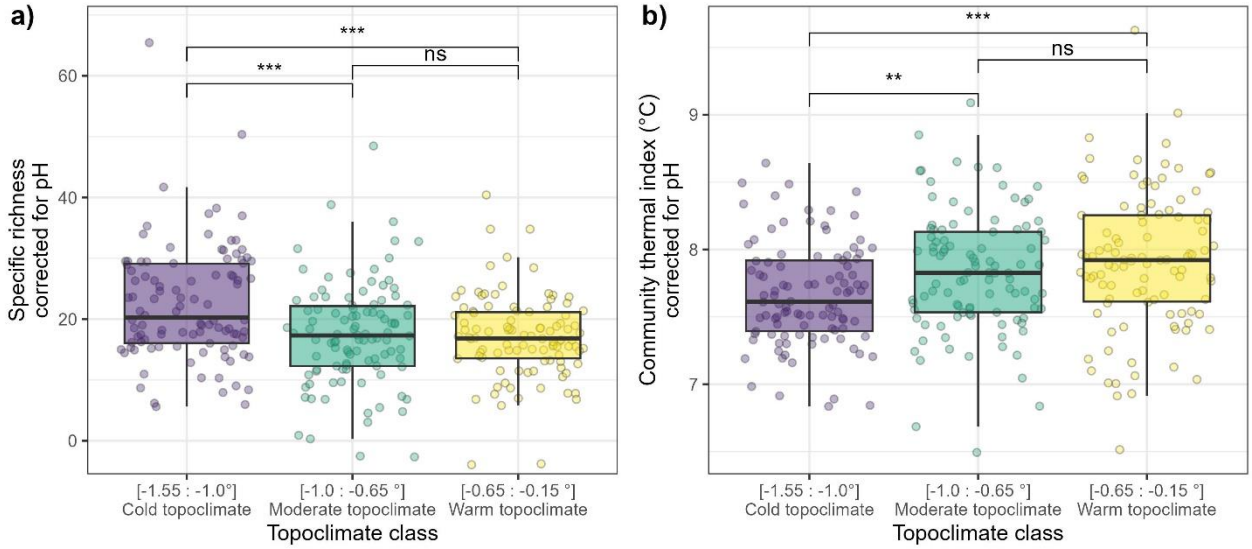

Figure 3: Species richness (a) and community thermal index (b), corrected for bioindicated pH, of 306 floristic surveys evenly spread into three topoclimatic cooling classes. The correction consists of extracting the residuals of a linear model with pH as a sole predictor, this process could thus lead to negative specific richness. The p-value significance of a Wilcoxon test between two classes is displayed as follows: (ns): p>0.05 (*): p<0.05(**): p<0.01 (***): P<0.001.

The decreases in CTI and the increase in species richness in the cold topoclimatic class were explained by a surplus of relatively cold-adapted species (i.e. with a species thermal optimum of 9 °C or less) (Figure 4.a). The plots (n=102) in cold topoclimates displayed in total more than 50 to 100 more occurrences of relatively cold-adapted species per thermal optimum classes (1°C) than the other two categories (Figure 4.a). The intermediate topoclimatic class (n=102) also had a higher number of cold-adapted species compared to the warm topoclimatic class (n=102) (Figure 4.a). The cold topoclimatic class displayed 300 more forest-specialist species occurrences (Heinken *et al.*, 2022) than the other warmer topoclimatic classes, whereas the occurrences of generalist species increased by 200 in total (Figure 4.b). We recorded a total of 246, 242 and 223 species (i.e., species pool) in the cold, intermediate and warm topoclimatic classes, respectively. A total of 58, 41, and 33 species were unique to the cold, intermediate and warm topoclimatic classes, respectively. This means that there is nestedness of species between communities, as shown in Figure S5.

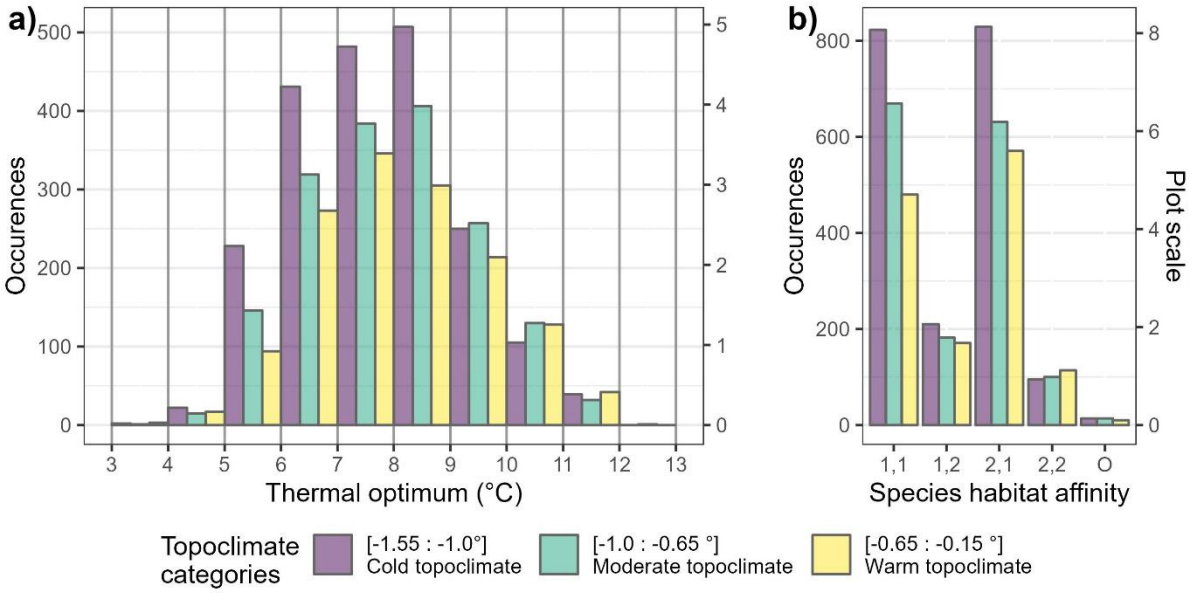

Figure 4: Occurrences of species in the three topoclimatic classes as a function of a) their thermal optimum (°C) and b) their habitat affinity defined by the EuForPlant list as follows: 1,1: closed forest mainly 1,2: forest edges and opening 2,1: forest and open vegetation 2,2: mainly in open vegetation (Heinken et al.*, 2022) The plot-scale occurrence of species is also shown (e.g., 400 occurrences corresponds to approximately 4 species per plots).*

4. Discussion

We found that both canopy cover and topographic factors strongly influenced understory temperature during the growing season. We disentangled the elevation gradient from the topoclimatic and microclimatic factors by estimating the lapse rate separately, which was expectably the main driver of understory temperature (Figure 2). After controlling for the lapse and pH, the temperature cooling by topographic factors, namely topoclimate, was the only significant driver of community composition and richness.

The positive correlation found between temperature and heat load can be attributed to the higher radiation an equator-facing slope receives, which increases both the mean and daily maximum temperature of the growing season in closed forests. This contrasts with a previous study which only found an effect of heat load on maximum temperature (Macek *et al.*, 2019). Alongside heat load, we found that topographic position influenced mean temperature so that ridges were warmer, and valley bottoms were cooler but had no effect on maximum temperature. We attribute this decrease in temperature to cold air pooling that occurs during nighttime, thus influencing mean daily temperature but with a minimal effect during the hottest hour of the day, when air temperature is homogeneously warm (Smith *et al.*, 2010; Vosper & Brown, 2008). The cooling effect of understory temperature by canopy cover was most apparent for maximum temperature but was also significant for mean temperature. These observations concur with studies with comparable sampling (Davis *et al.*, 2019; Macek *et al.*, 2019). We showed a strong effect of topoclimatic factors on community composition and richness but no contribution of microclimatic factors. Our

microclimatic model allowed us to separately predict the lapse rate, topoclimatic cooling and canopy cover cooling with mean temperature as a unit. This allows inferring direct links between temperature variation and communities, a necessary step to advance correlative studies.

The lack of correlation between species richness or community composition (climatic affinity) with microclimatic cooling is surprising as a majority of studies conducted in lowland forests concluded that dense canopy cover (or closure) explains both the assembly of communities and their slow temporal response to climate change (De Frenne *et al.*, 2013, 2019; Maclean *et al.*, 2015; Richard *et al.*, 2021; Zellweger *et al.*, 2020). In mountain forests, however, the contribution of canopy cover to understory temperature is still under scrutiny (Davis *et al.*, 2019; Macek *et al.*, 2019; Zellweger, Coomes, *et al.*, 2019). We found that topoclimatic factors outweighed canopy closure in explaining understory temperature in our study area (that harbors limited canopy closure variation and high topographic variation), which may explain the absence of a link between canopy cover and communities. This finding adds to the current divergent results from Macek *et al.*, (2019) who found no effect of canopy and Vandewiele *et al.*, (2023) who found a predominance of canopy control on temperature in mountain forests. These apparent contrasting results illustrate the complexity and interactions of factors in mountain forest microclimates, potentially depending on site-specific variations in topography and canopy cover, alongside with synoptic conditions leading to difference in transmittance.

Part of the challenge to determine canopy cover controls in mountain forests stems from the myriads of methods that are used to estimate canopy cover, ranging from hemispheric photographs, and terrestrial lidar-derived metrics to remotely sensed canopy cover estimations (Ma *et al.*, 2017; Zellweger, De Frenne, *et al.*, 2019). We used Copernicus tree density 2018 satellite images to calibrate the microclimatic model and predict its buffering effect on communities. Remote sensed tree closure density does not account for the vertical profile of trees, which have profound influence on sunlight interception and consequently on understory temperatures (Gril *et al.*, 2023; Zellweger, Coomes, *et al.*, 2019). Remotely sensed canopy cover was significantly but poorly correlated with our field measures (visual estimation and photography), and the year of remote sensing (2018) does not match the average year of a floristic survey (2015.6). These inaccuracies and the missing link of the forest vertical profile could partly explain the lack of a significant relationship between community compositions and cooling induced by canopy cover. We fitted additional understory temperature models with *in situ* measurements of canopy cover to conservatively reject canopy cover as a prominent driver of microclimate and consequently community composition. These models showed no correlation between understory temperatures and canopy closure except for the interaction between immediate canopy closure (photography) in equator-facing slopes (Table S2, Table S3). This demonstrates the need to simultaneously study multiple microclimatic drivers and their interactions in mountain ranges (Davis *et al.*, 2019; Greiser *et al.*, 2020).

We found that temperature variation owing to topography was equally important in shaping a community's affinity to climate compared to that of the elevational gradient (Table 2, after soil pH has been controlled for). This is understandably a consequence of community assembly dictated in part by the environment. Lower temperatures at higher altitudes or in topographically shaded slopes can exert a selection pressure on species not adapted to cold whereas lower elevation and high radiation slopes select species not sensitive to late freezing and adapted to warmer temperatures (Figure 3). Our prediction of both elevation and topography control on mean temperature are quantified the same unit, Celsius degrees °C, but topography-induced temperature effect on community composition is fourfold compared to that of elevation (Table 2). This implies that mean temperature alone cannot drive the difference in community composition, and other biophysical factors correlated with topography-induced temperature should be at play. Maximum temperature could be a better predictor of the crossing of physiological thresholds dictating species selection (Macek *et al.*, 2019; Pérez-Navarro *et al.*, 2021). However, this hypothesis could not be tested with our dataset as mean and maximum understory temperature were highly correlated. Soil moisture and vapor pressure deficit can also explain the important contribution of topography to communities (Davis *et al.*, 2019).

Our topographic position metric relies on hydrography, demonstrating that cold air pooling could occur alongside wetter soils and synergistically favor cold-adapted species not tolerant to drought (Bénichou & Le Breton, 1987; Finocchiaro *et al.*, 2023; Raduła *et al.*, 2018). Conversely, ridges and south-facing slopes exacerbate the effect of warmer temperatures by desiccation, via stronger winds and evaporation, respectively (Davis *et al.*, 2019; Piedallu *et al.*, 2023; Rita *et al.*, 2021). These factors altogether and the differences we found in contribution to community composition (Table 2) challenge the use of a single microclimate variable (e.g., mean temperature) to predict community patterns and species distribution. Explicitly considering other microscale biophysical factors in a multivariate fashion (Pérez-Navarro *et al.*, 2021), the improvement of mechanistic modeling of microclimate (Maclean, 2020) could improve predictions of present and future community composition.

The cold-adapted communities we observed in cold topoclimates are the result of an increase in relatively cold-adapted species occurrences rather than of a decrease in relatively warm-adapted species (Figure 3). This hints that the constraints on community assembly, in our study region, are a result of temperature becoming too warm for cold-adapted species, rather than otherwise. This increase in occurrences explains the higher specific richness in cold topoclimates (Figure 3). Canopy cover has been identified as the driver of the diversity of many taxa in lowland forests due to its buffering of microclimate and light interception (Tinya *et al.*, 2021; Zellweger *et al.*, 2015). Its lower contribution to microclimate variation in mountain forests and the limitation in its measurement mentioned earlier may explain why we do not detect this pattern. Further to an understory cooling, colder topoclimates could also increase moisture, thus alleviating competition for water

during summer and allowing more species to co-occur (Raduła *et al.*, 2018; Sanczuk *et al.*, 2022).

How these local cooler and wetter conditions are decoupled from the climate warming trend is of utmost importance as they allow for the persistence of cold-adapted species (Greiser *et al.*, 2020; Lenoir *et al.*, 2017), or provide opportunities to facilitate colonization thus facilitating range shifts (Serra-Diaz *et al.*, 2015). The thermal heterogeneity topoclimate produced in mountain ranges (Figure 2) should also be considered as a driver of landscape-scale diversity (Stein *et al.*, 2014) and a potential source of community adaptation because species of diverging climatic adaptation coexist in a relatively small area (Hylander *et al.*, 2022; Lenoir *et al.*, 2013). More specifically, our results support the "identifying and protecting microrefugia" section highlighted by Hylander *et al.*, (2022), as north-facing slopes and topographic depressions are easily identifiable from maps, and their cooling capacities and cold-adapted communities confirmed by visits to the field. Although we didn't find a significant canopy variation contribution, canopy is essential to create the ultimate understory condition and should be preserved to take advantage of the topoclimate. This could be achieved through selective logging and continuous cover silviculture and the reduction of edge effects thanks to buffer zones around the microrefugia. Conservation targeting cold topoclimates is more robust because of the increase in redundancy and biodiversity those locations provide (Table S5). Additionally, maintaining a connected forest will foster the benefits of the thermal heterogeneity created by topography (Hylander *et al.*, 2022). Indeed, warm topoclimates will serve as source populations of species adapted to the current climate, and cold topoclimates will maintain cold-adapted populations, resulting in a heterogenous landscape.

In summary, we show that elevation, topography, and to a lesser extent, canopy closure determines growing season understory temperature in the Vosges mountains in France. Besides elevation, the contribution of topoclimate was the main predictor of community composition and diversity. Understory plant communities of cold topoclimates (north-facing slopes and valley bottoms) harbored a higher number of generalist and forest specialist cold-adapted species. Our results place topography as a prominent driver of forest temperature and a key factor to consider for protecting forest cold-adapted species in the context of accelerated global warming.

5. Data availability

The spatial, microclimatic, and floristic data used for this analysis can be found in the repository: https://github.com/Jeremy-borderieux/Article_microclim_vosges along with the R script that can be used to reproduce the analyses and the figures, under the DOI https://doi.org/10.5281/zenodo.12626861.

6. Acknowledgment

The authors are grateful to the Grand Ventron naturel reserve and its director Laurent Domergue for the permission to access the core of the protected forest. The authors acknowledge the National Office for Forests (ONF) for permission to place loggers in public forests. The authors thank the AgroParisTech students and professors involved in the collection of floristic data. The authors thank the funding from a PHC Tournesol mobility grant N° 47550SB. JB Acknowledge the funding from a joint funding from Region Grand Est and AgroParisTech (19_GE8_01020p05035). JMSD was funded by the ANR-JCJC (Agence Nationale de la Recherche, jeunes chercheuses et jeunes chercheurs) SEEDFOR (ANR-21-CE32-0003). JMSD acknowledges the support from NASA for UConn's Ecological Modelling Institute (#80NSSC 22K0883).

7. References

Ashcroft, M. B. (2010). Identifying refugia from climate change : Identifying refugia from climate change. *Journal of Biogeography*. https://doi.org/10.1111/j.1365-2699.2010.02300.x

Ashcroft, M., Chisholm, L., & French, K. (2008). The effect of exposure on landscape scale soil surface temperatures and species distribution models. *Faculty of Science - Papers (Archive)*, 211-225. https://doi.org/10.1007/s10980-007-9181-8

Barbosa, A. M., Real, R., Munoz, A. R., & Brown, J. A. (2013). New measures for assessing model equilibrium and prediction mismatch in species distribution models. *Diversity and Distributions*, *19*(10), 1333-1338. https://doi.org/10.1111/ddi.12100

Bénichou, P., & Le Breton, O. (1987). Prise en compte de la topographie pour la cartographie de champs pluviométriques statistiques : La méthode Aurelhy. *Colloques de l'INRA*, *39*(51-69).

Borderieux, J., Gégout, J.-C., & Serra-Diaz, J. M. (2023). High landscape-scale forest cover favours cold-adapted plant communities in agriculture–forest mosaics. *Global Ecology and Biogeography*, *32*(6), 893-903. https://doi.org/10.1111/geb.13676

Bramer, I., Anderson, B. J., Bennie, J., Bladon, A. J., De Frenne, P., Hemming, D., Hill, R. A., Kearney, M. R., Körner, C., Korstjens, A. H., Lenoir, J., Maclean, I. M. D., Marsh, C. D., Morecroft, M. D., Ohlemüller, R., Slater, H. D., Suggitt, A. J., Zellweger, F., & Gillingham, P. K. (2018). Chapter Three—Advances in Monitoring and Modelling Climate at Ecologically Relevant Scales. In D. A. Bohan, A. J. Dumbrell, G. Woodward, & M. Jackson (Éds.), *Advances in Ecological Research* (Vol. 58, p. 101-161). Academic Press. https://doi.org/10.1016/bs.aecr.2017.12.005

Copernicus. (2018). *High Resolution Layer Tree Cover Density* [Data set]. https://land.copernicus.eu/en/products/high-resolution-layer-tree-cover-density

Davis, F. W., Synes, N. W., Fricker, G. A., McCullough, I. M., Serra-Diaz, J. M., Franklin, J., & Flint, A. L. (2019). LiDAR-derived topography and forest structure predict fine-scale variation in daily surface temperatures in oak savanna and conifer forest landscapes. *Agricultural and Forest Meteorology*, *269-270*, 192-202. https://doi.org/10.1016/j.agrformet.2019.02.015

De Frenne, P., Lenoir, J., Luoto, M., Scheffers, B. R., Zellweger, F., Aalto, J., Ashcroft, M. B., Christiansen, D. M., Decocq, G., De Pauw, K., Govaert, S., Greiser, C., Gril, E., Hampe, A., Jucker, T., Klinges, D. H., Koelemeijer, I. A., Lembrechts, J. J., Marrec, R., … Hylander, K. (2021). Forest microclimates and climate change : Importance, drivers and future research agenda. *Global Change Biology*. https://doi.org/10.1111/gcb.15569

De Frenne, P., Rodriguez-Sanchez, F., Coomes, D. A., Baeten, L., Verstraeten, G., Vellend, M., Bernhardt-Romermann, M., Brown, C. D., Brunet, J., Cornelis, J., Decocq, G. M., Dierschke, H., Eriksson, O., Gilliam, F. S., Hedl, R., Heinken, T., Hermy, M., Hommel, P., Jenkins, M. A., … Verheyen, K. (2013). Microclimate moderates plant responses to macroclimate warming. *Proceedings of the National Academy of Sciences*, *110*(46), 18561-18565. https://doi.org/10.1073/pnas.1311190110

De Frenne, P., Zellweger, F., Rodríguez-Sánchez, F., Scheffers, B. R., Hylander, K., Luoto, M., Vellend, M., Verheyen, K., & Lenoir, J. (2019). Global buffering of temperatures under forest canopies. *Nature Ecology & Evolution*, *3*(5), 744-749. https://doi.org/10.1038/s41559-019-0842-1

Degen, T., Devillez, F., & Jacquemart, A.-L. (2005). Gaps promote plant diversity in beech forests (Luzulo-Fagetum), North Vosges, France. *Annals of Forest Science*, *62*(5), 429-440. https://doi.org/10.1051/forest:2005039

Dietz, L., Collet, C., Dupouey, J.-L., Lacombe, E., Laurent, L., & Gégout, J.-C. (2020). Windstorm-induced canopy openings accelerate temperate forest adaptation to global warming. *Global Ecology and Biogeography*. https://doi.org/10.1111/geb.13177

Dobrowski, S. Z. (2011). A climatic basis for microrefugia : The influence of terrain on climate. *Global Change Biology*, *17*(2), 1022-1035. https://doi.org/10.1111/j.1365-2486.2010.02263.x

Dunnington, D., & Thorne, B. (2020). ggspatial : Spatial Data Framework for ggplot2. *R package version1*, *1*.

Ellis, C. J., & Eaton, S. (2021). Climate change refugia : Landscape, stand and tree-scale microclimates in epiphyte community composition. *The Lichenologist*, *53*(1), 135-148. https://doi.org/10.1017/S0024282920000523

Evans, J. S., & Murphy, M. A. (2021). *spatialEco*. https://github.com/jeffreyevans/spatialEco

Finocchiaro, M., Médail, F., Saatkamp, A., Diadema, K., Pavon, D., & Meineri, E. (2023). Bridging the gap between microclimate and microrefugia : A bottom-up approach reveals strong climatic and biological offsets. *Global Change Biology*, *29*(4), 1024-1036. https://doi.org/10.1111/gcb.16526

Franklin, J., Davis, F. W., Ikegami, M., Syphard, A. D., Flint, L. E., Flint, A. L., & Hannah, L. (2013). Modeling plant species distributions under future climates : How fine scale do climate projections need to be? *Global Change Biology*, *19*(2), 473-483. https://doi.org/10.1111/gcb.12051

Franklin, J., Serra-Diaz, J. M., Syphard, A. D., & Regan, H. M. (2016). Global change and terrestrial plant community dynamics. *Proceedings of the National Academy of Sciences*, *113*(14), 3725-3734. https://doi.org/10.1073/pnas.1519911113

Gargominy, O. (2022). *TAXREF v13.0, référentiel taxonomique pour la France*. [Data set]. UMS PatriNat (OFB-CNRS-MNHN), Paris. https://doi.org/10.15468/VQUEAM

Gégout, J.-C., Coudun, C., Bailly, G., & Jabiol, B. (2005). EcoPlant : A forest site database linking floristic data with soil and climate variables. *Journal of Vegetation Science*, *16*(2), 257-260. https://doi.org/10.1111/j.1654-1103.2005.tb02363.x

Greiser, C., Ehrlén, J., Meineri, E., & Hylander, K. (2020). Hiding from the climate : Characterizing microrefugia for boreal forest understory species. *Global Change Biology*, *26*(2), 471-483. https://doi.org/10.1111/gcb.14874

Gril, E., Laslier, M., Gallet-Moron, E., Durrieu, S., Spicher, F., Le Roux, V., Brasseur, B., Haesen, S., Van Meerbeek, K., Decocq, G., Marrec, R., & Lenoir, J. (2023). Using airborne LiDAR to map forest microclimate temperature buffering or amplification. *Remote Sensing of Environment*, *298*, 113820. https://doi.org/10.1016/j.rse.2023.113820

Gudiksen, P. H., Leone, J. M., King, C. W., Ruffieux, D., & Neff, W. D. (1992). Measurements and Modeling of the Effects of Ambient Meteorology on Nocturnal Drainage Flows. *Journal of Applied Meteorology and Climatology*, *31*(9), 1023‑1032. https://doi.org/10.1175/1520-0450(1992)031<1023:MAMOTE>2.0.CO;2

Haesen, S., Lembrechts, J. J., De Frenne, P., Lenoir, J., Aalto, J., Ashcroft, M. B., Kopecký, M., Luoto, M., Maclean, I., Nijs, I., Niittynen, P., van den Hoogen, J., Arriga, N., Brůna, J., Buchmann, N., Čiliak, M., Collalti, A., De Lombaerde, E., Descombes, P., … Van Meerbeek, K. (2021). ForestTemp – Sub-canopy microclimate temperatures of European forests. *Global Change Biology*, *27*(23), 6307‑6319. https://doi.org/10.1111/gcb.15892

Haesen, S., Lenoir, J., Gril, E., Frenne, P. D., Lembrechts, J., Kopecký, M., Macek, M., Man, M., Wild, J., & Meerbeek, K. V. (2023). *Uncovering the hidden niche : Incorporating microclimate temperature into species distribution models*. https://ecoevorxiv.org/repository/view/5364/

Hannah, L., Flint, L., Syphard, A. D., Moritz, M. A., Buckley, L. B., & McCullough, I. M. (2014). Fine-grain modeling of species' response to climate change : Holdouts, stepping-stones, and microrefugia. *Trends in Ecology & Evolution*, *29*(7), 390‑397. https://doi.org/10.1016/j.tree.2014.04.006

Heinken, T., Diekmann, M., Liira, J., Orczewska, A., Schmidt, M., Brunet, J., Chytrý, M., Chabrerie, O., Decocq, G., De Frenne, P., Dřevojan, P., Dzwonko, Z., Ewald, J., Feilberg, J., Graae, B. J., Grytnes, J.-A., Hermy, M., Kriebitzsch, W.-U., Laiviņš, M., … Vanneste, T. (2022). The European Forest Plant Species List (EuForPlant) : Concept and applications. *Journal of Vegetation Science*, *33*(3), e13132. https://doi.org/10.1111/jvs.13132

Hijmans, R. J. (2020). *raster : Geographic Data Analysis and Modeling*. https://CRAN.R-project.org/package=raster

Hylander, K., Greiser, C., Christiansen, D. M., & Koelemeijer, I. A. (2022). Climate adaptation of biodiversity conservation in managed forest landscapes. *Conservation Biology*, *36*(3), e13847. https://doi.org/10.1111/cobi.13847

IGN. (2013). *Fiches descriptives des grandes régions écologiques (GRECO) et des sylvoécorégions (SER)*. https://inventaire-forestier.ign.fr/spip.php?article773

IGN. (2017). *BD ALTI Le modèle numérique de terrain (MNT) maillé qui décrit le relief du territoire français à moyenne échelle* [Data set]. https://geoservices.ign.fr/documentation/donnees/alti/bdalti

IGN. (2019). *BD Forêt version 2*. Institut National de l'Information Géographique et Forestière. https://inventaire-forestier.ign.fr/spip.php?article646

IPCC. (2021). Summary for Policymakers. In V. Masson-Delmotte, P. Zhai, A. Pirani, S. L. Connors, C. Péan, S. Berger, N. Caud, Y. Chen, L. Goldfarb, M. I. Gomis, M. Huang, K. Leitzell, E. Lonnoy, J. B. R. Matthews, T. K. Maycock, T. Waterfield, O. Yelekçi, R. Yu, & B. Zhou (Éds.), *Climate Change 2021 : The Physical Science Basis. Contribution of Working Group I to the Sixth Assessment Report of the Intergovernmental Panel on Climate Change* (p. 3‑32). Cambridge University Press. https://doi.org/10.1017/9781009157896.001

Johnston, A. K., Brewster, D., & Berghaus, H. K. W. (1848). *The physical atlas : A series of maps & notes illustrating the geographical distribution of natural phenomena* [Map]. William Blackwood & Sons.

Kemppinen, J., Lembrechts, J. J., Van Meerbeek, K., Carnicer, J., Chardon, N. I., Kardol, P., Lenoir, J., Liu, D., Maclean, I., Pergl, J., Saccone, P., Senior, R. A., Shen, T., Słowińska, S., Vandvik, V., von Oppen, J., Aalto, J., Ayalew, B., Bates, O., … De Frenne, P. (2023). *Microclimate, an inseparable part of ecology and biogeography*. Zenodo. https://doi.org/10.5281/zenodo.7973314

687 Koerner, W., Dupouey, J. L., Dambrine, E., & Benoit, M. (1997). Influence of Past Land Use
688 on the Vegetation and Soils of Present Day Forest in the Vosges Mountains, France.
689 *Journal of Ecology*, *85*(3), 351-358. https://doi.org/10.2307/2960507
690 Lembrechts, J. J., Lenoir, J., Scheffers, B., & De Frenne, P. (2021). Designing countrywide
691 and regional microclimate networks. *Global Ecology and Biogeography*.
692 https://doi.org/10.1111/geb.13290
693 Lenoir, J., Graae, B. J., Aarrestad, P. A., Alsos, I. G., Armbruster, W. S., Austrheim, G.,
694 Bergendorff, C., Birks, H. J. B., Bråthen, K. A., Brunet, J., Bruun, H. H., Dahlberg,
695 C. J., Decocq, G., Diekmann, M., Dynesius, M., Ejrnæs, R., Grytnes, J.-A., Hylander,
696 K., Klanderud, K., … Svenning, J.-C. (2013). Local temperatures inferred from plant
697 communities suggest strong spatial buffering of climate warming across Northern
698 Europe. *Global Change Biology*, *19*(5), 1470-1481.
699 https://doi.org/10.1111/gcb.12129
700 Lenoir, J., Hattab, T., & Pierre, G. (2017). Climatic microrefugia under anthropogenic
701 climate change : Implications for species redistribution. *Ecography*, *40*(2), 253-266.
702 https://doi.org/10.1111/ecog.02788
703 Ma, Q., Su, Y., & Guo, Q. (2017). Comparison of Canopy Cover Estimations From Airborne
704 LiDAR, Aerial Imagery, and Satellite Imagery. *IEEE Journal of Selected Topics in*
705 *Applied Earth Observations and Remote Sensing*, *10*(9), 4225-4236.
706 https://doi.org/10.1109/JSTARS.2017.2711482
707 Macek, M., Kopecký, M., & Wild, J. (2019). Maximum air temperature controlled by
708 landscape topography affects plant species composition in temperate forests.
709 *Landscape Ecology*, *34*(11), 2541-2556. https://doi.org/10.1007/s10980-019-00903-x
710 Maclean, I. M. D. (2020). Predicting future climate at high spatial and temporal resolution.
711 *Global Change Biology*, *26*(2), 1003-1011. https://doi.org/10.1111/gcb.14876
712 Maclean, I. M. D., Hopkins, J. J., Bennie, J., Lawson, C. R., & Wilson, R. J. (2015).
713 Microclimates buffer the responses of plant communities to climate change. *Global*
714 *Ecology and Biogeography*, *24*(11), 1340-1350. https://doi.org/10.1111/geb.12359
715 Man, M., Kalčík, V., Macek, M., Brůna, J., Hederová, L., Wild, J., & Kopecký, M. (2023).
716 myClim : Microclimate data handling and standardised analyses in R. *Methods in*
717 *Ecology and Evolution*, *14*(9). https://doi.org/10.1111/2041-210X.14192
718 McCune, B., & Keon, D. (2002). Equations for potential annual direct incident radiation and
719 heat load. *Journal of Vegetation Science*, *13*(4), 603-606.
720 https://doi.org/10.1111/j.1654-1103.2002.tb02087.x
721 McLaughlin, B. C., Ackerly, D. D., Klos, P. Z., Natali, J., Dawson, T. E., & Thompson, S. E.
722 (2017). Hydrologic refugia, plants, and climate change. *Global Change Biology*, *23*(8),
723 2941-2961. https://doi.org/10.1111/gcb.13629
724 Météo France. (2024). *Meteo.data.gouv.fr*. https://meteo.data.gouv.fr/datasets
725 Pastore, M. A., Classen, A. T., D'Amato, A. W., Foster, J. R., & Adair, E. C. (2022). Cold-air
726 pools as microrefugia for ecosystem functions in the face of climate change. *Ecology*,
727 *103*(8), e3717. https://doi.org/10.1002/ecy.3717
728 Pebesma, E. (2018). Simple Features for R: Standardized Support for Spatial Vector Data.
729 *The R Journal*, *10*(1), 439-446. https://doi.org/10.32614/RJ-2018-009
730 Pérez-Navarro, M. Á., Serra-Diaz, J. M., Svenning, J., Esteve-Selma, M. Á., Hernández-
731 Bastida, J., & Lloret, F. (2021). Extreme drought reduces climatic disequilibrium in
732 dryland plant communities. *Oikos*. https://doi.org/10.1111/oik.07882
733 Piedallu, C., Dallery, D., Bresson, C., Legay, M., Gégout, J.-C., & Pierrat, R. (2023). Spatial
734 vulnerability assessment of silver fir and Norway spruce dieback driven by climate
735 warming. *Landscape Ecology*, *38*(2), 341-361. https://doi.org/10.1007/s10980-022-
736 01570-1

Piqué, A., Pluck, P., Schneider, J.-L., & Whitechurch, H. (1994). The Vosges Massif. In J. Chantraine, J. Rolet, D. S. Santallier, A. Piqué, & J. D. Keppie (Éds.), *Pre-Mesozoic Geology in France and Related Areas* (p. 416-425). Springer. https://doi.org/10.1007/978-3-642-84915-2_32

R Core Team. (2019). *R: A Language and Environment for Statistical Computing*. R Foundation for Statistical Computing. https://www.R-project.org/

Raduła, M. W., Szymura, T. H., & Szymura, M. (2018). Topographic wetness index explains soil moisture better than bioindication with Ellenberg's indicator values. *Ecological Indicators*, *85*, 172-179. https://doi.org/10.1016/j.ecolind.2017.10.011

Rey, D., & Neuhäuser, M. (2011). Wilcoxon-Signed-Rank Test. In M. Lovric (Éd.), *International Encyclopedia of Statistical Science* (p. 1658-1659). Springer. https://doi.org/10.1007/978-3-642-04898-2_616

Richard, B., Dupouey, J.-L., Corcket, E., Alard, D., Archaux, F., Aubert, M., Boulanger, V., Gillet, F., Langlois, E., Macé, S., Montpied, P., Beaufils, T., Begeot, C., Behr, P., Boissier, J.-M., Camaret, S., Chevalier, R., Decocq, G., Dumas, Y., … Lenoir, J. (2021). The climatic debt is growing in the understorey of temperate forests : Stand characteristics matter. *Global Ecology and Biogeography*, *30*(7). https://doi.org/10.1111/geb.13312

Rita, A., Bonanomi, G., Allevato, E., Borghetti, M., Cesarano, G., Mogavero, V., Rossi, S., Saulino, L., Zotti, M., & Saracino, A. (2021). Topography modulates near-ground microclimate in the Mediterranean Fagus sylvatica treeline. *Scientific Reports*, *11*(1), 8122. https://doi.org/10.1038/s41598-021-87661-6

Sala, O. E., Chapin, F. S., Armesto, J. J., Berlow, E., Bloomfield, J., Dirzo, R., Huber-Sanwald, E., Huenneke, L. F., Jackson, R. B., Kinzig, A., Leemans, R., Lodge, D. M., Mooney, H. A., Oesterheld, M., Poff, N. L., Sykes, M. T., Walker, B. H., Walker, M., & Wall, D. H. (2000). Global biodiversity scenarios for the year 2100. *Science (New York, N.Y.)*, *287*(5459), 1770-1774. https://doi.org/10.1126/science.287.5459.1770

Sanczuk, P., De Lombaerde, E., Haesen, S., Van Meerbeek, K., Luoto, M., Van der Veken, B., Van Beek, E., Hermy, M., Verheyen, K., Vangansbeke, P., & De Frenne, P. (2022). Competition mediates understorey species range shifts under climate change. *Journal of Ecology*, *110*(8), 1813-1825. https://doi.org/10.1111/1365-2745.13907

Sannier, C., Gallego, J., Langanke, T., Donezar, U., & Pennec, A. (2023). Tree cover area estimation in europe based on the combination of in situ reference data and the copernicus high resolution layer on tree cover density. *The International Archives of the Photogrammetry, Remote Sensing and Spatial Information Sciences*, *XLVIII-M-1-2023*, 277-284. https://doi.org/10.5194/isprs-archives-XLVIII-M-1-2023-277-2023

Schweiger, A. H., Irl, S. D. H., Steinbauer, M. J., Dengler, J., & Beierkuhnlein, C. (2016). Optimizing sampling approaches along ecological gradients. *Methods in Ecology and Evolution*, *7*(4), 463-471. https://doi.org/10.1111/2041-210X.12495

Serra-Diaz, J. M., Scheller, R. M., Syphard, A. D., & Franklin, J. (2015). Disturbance and climate microrefugia mediate tree range shifts during climate change. *Landscape Ecology*, *30*(6), 1039-1053. https://doi.org/10.1007/s10980-015-0173-9

Smith, S. A., Brown, A. R., Vosper, S. B., Murkin, P. A., & Veal, A. T. (2010). Observations and Simulations of Cold Air Pooling in Valleys. *Boundary-Layer Meteorology*, *134*(1), 85-108. https://doi.org/10.1007/s10546-009-9436-9

Stein, A., Gerstner, K., & Kreft, H. (2014). Environmental heterogeneity as a universal driver of species richness across taxa, biomes and spatial scales. *Ecology Letters*, *17*(7), 866-880. https://doi.org/10.1111/ele.12277

Thomas, A. L., Dambrine, E., King, D., Party, J. P., & Probst, A. (1999). A spatial study of the relationships between streamwater acidity and geology, soils and relief (Vosges, northeastern France). *Journal of Hydrology*, *217*(1), 35-45. https://doi.org/10.1016/S0022-1694(99)00014-1

Tichý, L. (2016). Field test of canopy cover estimation by hemispherical photographs taken with a smartphone. *Journal of Vegetation Science*, *27*(2), 427-435. https://doi.org/10.1111/jvs.12350

Tinya, F., Kovács, B., Bidló, A., Dima, B., Király, I., Kutszegi, G., Lakatos, F., Mag, Z., Márialigeti, S., Nascimbene, J., Samu, F., Siller, I., Szél, G., & Ódor, P. (2021). Environmental drivers of forest biodiversity in temperate mixed forests – A multi-taxon approach. *Science of The Total Environment*, *795*, 148720. https://doi.org/10.1016/j.scitotenv.2021.148720

Vandewiele, M., Geres, L., Lotz, A., Mandl, L., Richter, T., Seibold, S., Seidl, R., & Senf, C. (2023). Mapping spatial microclimate patterns in mountain forests from LiDAR. *Agricultural and Forest Meteorology*, *341*, 109662. https://doi.org/10.1016/j.agrformet.2023.109662

Vangansbeke, P., Máliš, F., Hédl, R., Chudomelová, M., Vild, O., Wulf, M., Jahn, U., Welk, E., Rodríguez-Sánchez, F., & Frenne, P. D. (2021). ClimPlant : Realized climatic niches of vascular plants in European forest understoreys. *Global Ecology and Biogeography*, *30*(6), 1183-1190. https://doi.org/10.1111/geb.13303

Vosper, S. B., & Brown, A. R. (2008). Numerical Simulations of Sheltering in Valleys : The Formation of Nighttime Cold-Air Pools. *Boundary-Layer Meteorology*, *127*(3), 429-448. https://doi.org/10.1007/s10546-008-9272-3

Wickham, H. (2011). Ggplot2. *WIREs Computational Statistics*, *3*(2), 180-185. https://doi.org/10.1002/wics.147

Wiens, J. J. (2016). Climate-Related Local Extinctions Are Already Widespread among Plant and Animal Species. *PLOS Biology*, *14*(12), e2001104. https://doi.org/10.1371/journal.pbio.2001104

Wild, J., Kopecký, M., Macek, M., Šanda, M., Jankovec, J., & Haase, T. (2019). Climate at ecologically relevant scales : A new temperature and soil moisture logger for long-term microclimate measurement. *Agricultural and Forest Meteorology*. https://doi.org/10.1016/j.agrformet.2018.12.018

Zellweger, F., Braunisch, V., Morsdorf, F., Baltensweiler, A., Abegg, M., Roth, T., Bugmann, H., & Bollmann, K. (2015). Disentangling the effects of climate, topography, soil and vegetation on stand-scale species richness in temperate forests. *Forest Ecology and Management*, *349*, 36-44. https://doi.org/10.1016/j.foreco.2015.04.008

Zellweger, F., Coomes, D., Lenoir, J., Depauw, L., Maes, S. L., Wulf, M., Kirby, K. J., Brunet, J., Kopecký, M., Máliš, F., Schmidt, W., Heinrichs, S., den Ouden, J., Jaroszewicz, B., Buyse, G., Spicher, F., Verheyen, K., & De Frenne, P. (2019). Seasonal drivers of understorey temperature buffering in temperate deciduous forests across Europe. *Global Ecology and Biogeography*, *28*(12), 1774-1786. https://doi.org/10.1111/geb.12991

Zellweger, F., De Frenne, P., Lenoir, J., Rocchini, D., & Coomes, D. (2019). Advances in Microclimate Ecology Arising from Remote Sensing. *Trends in Ecology & Evolution*, *34*(4), 327-341. https://doi.org/10.1016/j.tree.2018.12.012

Zellweger, F., De Frenne, P., Lenoir, J., Vangansbeke, P., Verheyen, K., Bernhardt-Römermann, M., Baeten, L., Hédl, R., Berki, I., Brunet, J., Van Calster, H., Chudomelová, M., Decocq, G., Dirnböck, T., Durak, T., Heinken, T., Jaroszewicz, B., Kopecký, M., Máliš, F., … Coomes, D. (2020). Forest microclimate dynamics drive plant responses to warming. *Science*, *368*(6492), 772-775. https://doi.org/10.1126/science.aba6880

Zuur, A. F., & Ieno, E. N. (2016). A protocol for conducting and presenting results of regression-type analyses. *Methods in Ecology and Evolution*, *7*(6), 636-645. https://doi.org/10.1111/2041-210X.12577